Supplemental Data

Supplementary Materials and Methods

Patient samples

PBMCs were isolated by density gradient centrifugation with Histopaque (Sigma). Plasma was isolated from patients with CLL and age/sex matched healthy control subjects (Liverpool Lung Project Biobank), immediately following venepuncture, by centrifugation of EDTA anti-coagulated whole blood at 500x*g* for 5 minutes. The top 1 ml from the plasma layer was removed, without disturbing the leukocyte layer, and was snap frozen and then stored at -80^{o}C.

Total and unmethylated mtDNA quantification

Plasma was centrifuged sequentially at 500g for 10 min and 2000g for 10 min at room temperature to pellet cells and debris prior to extraction. Total DNA was isolated from 2 ml of plasma using the Qiamp MinElute ccfDNA kit (Qiagen, UK) using the suppliers' protocol. DNA was eluted in 40 μl of ddH_2O and stored in the freezer until use. Plasma cfDNA quantification was performed using real-time PCR to amplify the CCR5 gene and determining the C_t value (Qiagen Rotorgene, Germany). A standard curve was generated using in house genomic DNA standards, and test sample levels (genome equivalents/milliliter of plasma [GE/ml]) were determined from this. The plasma DNA yield was calculated by linear regression based on the standard curve.

The assay to detect unmethylated mtDNA was designed based on digesting DNA with the FspEI restriction endonuclease, which digests only methylated DNA, followed by a probe-based qPCR (Supplementary Figure 1). The assay design was selected to test for CpG but also non-CpG methylation in mtDNA, which is reported to be extensive (https://academic.oup.com/nar/article/47/19/10072/5563943). *In vitro* methylated DNA

(using SssI methylase, New England Biolabs) was used to test the efficiency and specificity of the assay.

Total mtDNA yield was quantified by absolute quantification PCR, without prior digestion of the DNA with FspEI. A standard curve of white blood cell DNA was used (0.155ng-40ng input). 2μl of the eluted DNA was used in the reaction; qPCR was performed in triplicate. For unmethylated mtDNA detection, 20μl of the eluted DNA was digested with 10U of FspEI (New England Biolabs) at 37°C overnight. Following endonuclease inactivation at 80 °C for 20 min, 4 μl of the digest was subjected to the qPCR assay using the Quantinova Probe PCR kit (Qiagen UK). Primer and probe sequences were the following: Fwd primer: 5' ACATTACAGTCAAATCCCTTCTC 3'; Rev primer: 5' GGAGCGAGGAGAGTAGCAC 3'; Probe: 5' FAM-TGCGGGATATTGATTTCACGGAG-BHQ1 3'. The reaction was performed on a StepOne real time PCR instrument (Applied Biosystems) with the following thermal profile: 95 °C for 2 min, 40 cycles consisted of 95 °C for 5 sec, 55 °C for 20 sec, 60 °C for 40 sec.

For unmethylated mtDNA calculation, the calibrator used was the mean value of the control samples and all values are expressed as a fold-change compared to this.

Surface and intracellular immunophenotyping

Surface labeling was as per the antibody manufacturer's instructions. For the FNA/PB staining a whole blood lysis/staining method was performed as per the manufacturer's instructions (eBiosciences). For each antigen the mean fluorescent intensity (MFI) of the $CD19^+/CD5^+$ CLL cells was recorded. For the p-STAT3/5 and p-p65 NF-κB measurement the cells were prepared using the True-Phos kit and protocol (Biolegend). Surface staining, including sTLR9, was performed prior to fixation to prevent labelling of eTLR9 following permeabilization. eTLR9

level staining was performed using the Cytofix/CytoPerm kit (Becton Dickinson) as per the manufacturer's instructions.

RNA-seq analysis

RNA quality control, mRNA TruSeq library generation was performed by Qiagen. Samples were sequenced using a 75-base single-end dual index read format on the Illumina® HiSeq2500 in high-output mode according to the manufacturer's instructions. Processing of raw RNA sequencing reads and subsequent differential gene expression analysis was then performed. Raw read data was converted to fastq format for all samples and reads were then trimmed of adapters and low quality read ends using Trim Galore (v0.5.0) software. Reads were mapped to the Gencode GRCh38 primary assembly reference genome, sourced from the Wellcome Sanger Institute server. Read counts, directly relating to the gene expression levels, were calculated by inferring library strand specificity from each sequence alignment file using RSeQC software, they were then summarized by feature, specifying strandedness, using FeatureCounts (v1.5.1) software. FeatureCounts was used both as part of a quality control strategy to identify outliers and batching effects and to assess read counts that were summarized at the exon, transcript and gene level. These read counts were taken forward for differential gene expression analysis using the R package: DESeq2. Subsequent gene ontology analysis of differentially expressed genes was performed using IPA analysis software (Qiagen).

qPCR of TLR9

RNA was reverse transcribed to cDNA using the High-Capacity cDNA Reverse Transcription Kit according to manufacturer's instructions (Applied Biosystems) and mixed with the TaqMan Fast Advanced Master Mix (Applied Biosystems). For the qPCR the TLR9 (Hs00370913_s1) and β-Actin (Hs99999903_m1) Taqman gene expression assays (Applied

Biosystems) were used. qPCR was performed in triplicate in three independent experiments using the AriaMx Real-time PCR System (Agilent) and the thermal profile: 50°C for 2 min, 95°C for 2 min, and then 40 cycles of 95°C for 1 s and 60°C for 20s. Expression data was normalized to the geometric mean of the house keeping gene and the -ΔCT calculated using the Agilent Aria MX software.

Xenotransplantation

CLL cells from 7 different patients were xenotransplanted into NOD/Shi-*scid*/IL-2Rγ^{null} (NSG) mice as previously described[31-33]. Mice were euthanised at time of illness typically associated with leukaemia in these murine models, namely: weight loss, hair loss, bulging eyes, loss of condition, hunched body, lethargy, reduced activity, pale feet, pinched face, piloerection, staggered gait, limping and occasional hind-leg paralysis. Furthermore, the murine phenotype at time of death was as previously reported[32-33] and included tumor in the blood, bone marrow and peritoneum. On occasion there was visual evidence of lesions in other organs including pancreas, kidney, liver. However, this was infrequent and generally infiltration was not detected in skin, lung or liver in these CLL models[33].

As per previous publications[32-33], splenic engraftment was measured using single cell suspensions prepared from murine spleens by Lymphoprep gradient centrifugation (Axis-Shield, Cheshire, UK) of cells generated by maceration of spleens through a wire mesh. These cells were labelled with fluorescently conjugated antibodies (Supplementary Table 1 panel G) and analysed using an LSRII with FACS Diva software (BD Biosciences) to determine CLL engraftment levels (hCD45^{+}CD19^{+}CD3^{-} cells) as a percentage of total cells.

Supplementary Table 1. List of antibody panels.

CLL Panel A (ODN2006/Plasma stimulation)		
Antibody	**Conjugate and clone**	**Supplier**
Anti-CD49d	PerCP-Cy5.5 9F10	Biolegend
Anti-CD38	APC HB-7	Biolegend
Anti-CD69	BV510 FN50	Biolegend
Anti-CD5	PE-Cy7 L17F12	Biolegend
Anti-CD19	Pacific Blue HIB	Biolegend
Viability dye	eFluor 780	eBioscience
CLL Panel B (surface and intracellular TLR9 on PB)		
Anti-TLR9	FITC 26C593.2	Imgenex
Anti-CD49d	PerCP-Cy5.5 9F10	Biolegend
Anti-CD38	APC HB-7	Biolegend
Anti-CD69	BV510 FN50	Biolegend
Anti-CD5	PE-Cy7 L17F12	Biolegend
Anti-CD19	Pacific Blue HIB	Biolegend
Viability dye	eFluor 780	eBioscience
CLL Panel C (surface TLR9 PB vs FNA).		
Anti-TLR9	APC eB72-1665	eBioscience
Anti-CD49d	PerCP-Cy5.5 9F10	Biolegend
Anti-CD38	FITC HB-7	Biolegend
Anti- CD69	BV510 FN50	Biolegend
Anti- CD5	PE-Cy7 L17F12	Biolegend
Anti- CD19	Pacific Blue HIB	Biolegend
Viability dye	eFluor 780	eBioscience
CLL Panel D (surface TLR9 blocking)		
Anti-TLR9	eB72-1665	eBioscience
Anti-CD49d	PerCP-Cy5.5 9F10	Biolegend
Anti-CD38	FITC HB-7	Biolegend
Anti- CD69	BV510 FN50	Biolegend
Anti- CD5	PE-Cy7 L17F12	Biolegend
Anti- CD19	Pacific Blue HIB	Biolegend
Viability dye	eFluor 780	eBioscience

CLL Panel E (p-STAT3, NF-κB p65 and p-STAT5***)***		
Anti-TLR9	FITC 26C593.2	Imgenex
Anti-CD49d	PerCP-Cy5.5 9F10	Biolegend
Anti-CD38	APC HB-7	Biolegend
Anti- CD5	PE-Cy7 L17F12	Biolegend
Anti- CD19	Pacific Blue HIB	Biolegend
Viability dye	eFluor 780	eBioscience
Anti-phospho-STAT3(Tyr705) or Anti-phospho-NF-κB p65 (Ser529) or Anti-phospho-STAT5 (Tyr694)	PE 13A3-1 PE B33B4WP PE A17016B	Biolegend ebiosciences Biolegend
CLL Panel F (Sorting)		
Anti- CD5	PE-Cy7 L17F12	Biolegend
Anti- CD19	Pacific Blue HIB	Biolegend
Viability dye	eFluor 520	eBioscience
Anti-TLR9	PE eB72-1665	eBioscience
Anti-CXCR4	AF-488 12G5	Novus Biologicals
CLL Panel G (Xenograft)		
Human Anti-CD45	Alexa Fluor 700 30-F11	eBioscience
Mouse Anti-CD45	eFluor 450 2D1	eBioscience
Human Anti-CD3	eFluor 780 SK7	eBioscience
Human Anti-CD19	PE-Cy7 HIB 19	eBioscience

Supplementary Table 2. Percentage of cells in the circulating versus migrated and lymph nodes versus peripheral blood. Circulating versus migrated are single counts due to low cell numbers in the migrated. LN versus PB are the mean of triplicate readings.

Patient	% sTLR9+ circulating	% sTLR9+ migrated
A	4.98	4.17
B	0.3	9.13
C	2.44	13.3
D	5.82	16.6
E	5.28	12.9
F	0.77	18.4
G	2.47	5.36
H	4.88	15.3
I	11.55	21.6
J	1.62	4.36

Patient	Mean % sTLR9+ PB	Mean % sTLR9+ LN
K	5.10	5.80
L	3.80	5.10
M	8.40	31.5
N	0.5	1.6
O	2.0	5.0
P	0.1	2.6
Q	1.5	1.7

Supplementary Figures

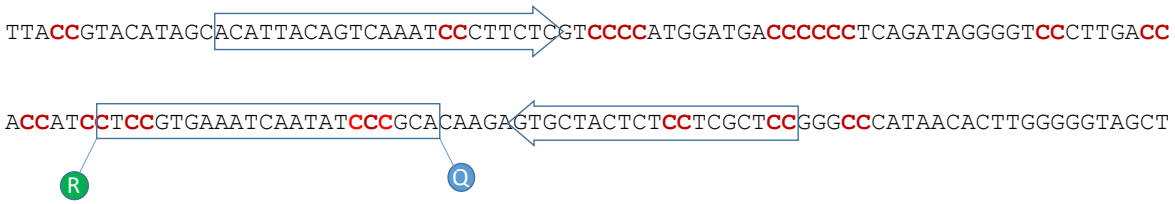

Supplementary Figure 1: Part of mtDNA sequence (D-loop region), which was used for the unmethylated mtDNA detection assay. FspEI recognicion sites (C^mC) are highlighted in red text. Primer and probe annealing sites for the qPCR assay are denoted with arrows and box in respect. Methylated DNA is digested by FspEI, therefore not resulting in a product in the subsequent qPCR.

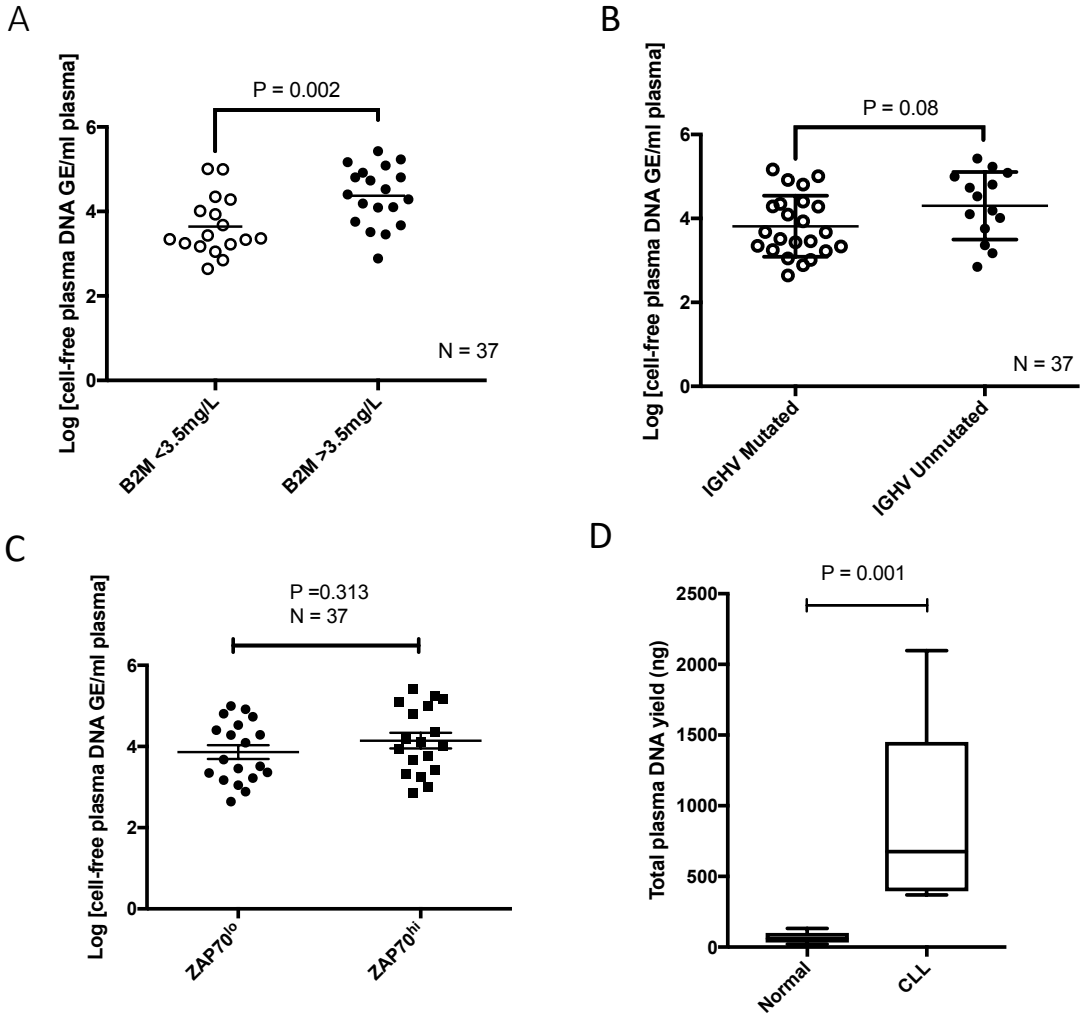

Supplementary Figure 2: Patients with CLL have raised levels of plasma DNA compared to healthy controls and these correlate with high B2M but not ZAP-70

Levels of cell-free DNA were measured in the plasma of 37 patients with a confirmed diagnosis of CLL. **(A)** Patients with >3.5mg/L serum B2M had higher levels of plasma DNA. **(B)** There was a trend towards higher levels in patients with unmutated IGHV compared to mutated. **(C)** Patients were classified as high ($ZAP70^{hi}$) or low ($ZAP70^{lo}$) using the clinically applicable 10% cut off. There was no correlation between the levels of cell-free DNA and percentage of ZAP-70 positive CLL cells. **(D)** Total mtDNA was quantified in the plasma of CLL patients (n=15) and healthy controls (n=27).The plasma from patients with CLL had a mean of 12.9-fold more mtDNA than that of the healthy controls.

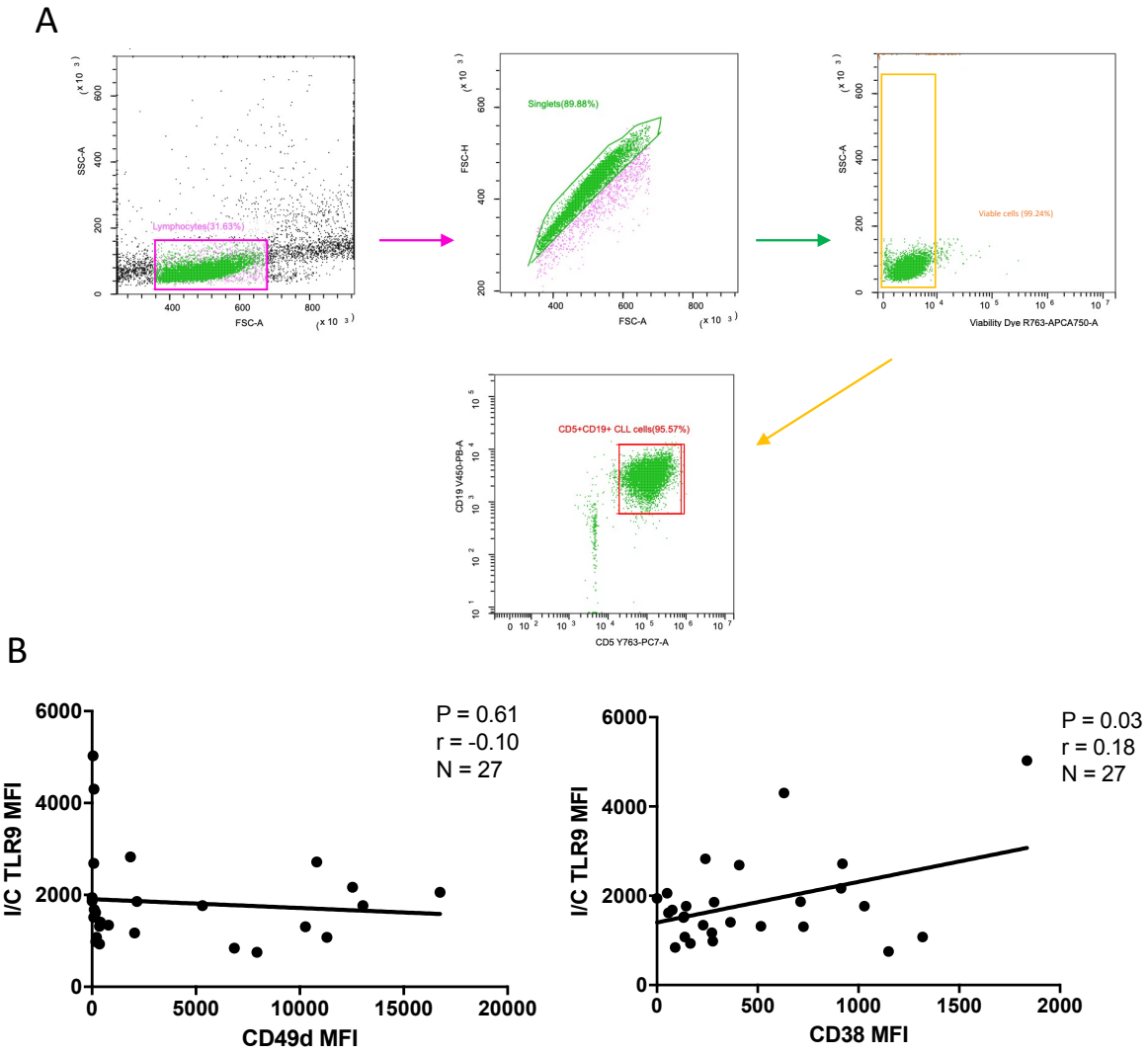

Supplementary Figure 3: Minor correlation between intracellular TLR9 with CD38 and none with CD49d using CD19+CD5+ gating strategy. Unstimulated primary PBMCs from 27 CLL patients were stained with antibodies to CD5, CD19, CD38, CD49d and a viability dye and then permeabilized and stained for intracellular TLR9 prior to flow cytometry. **(A)** A representative figure showing the strategy used for the identification and gating of viable CD5+CD19+ CLL cells. **(B)** CLL cells were gated on and the MFI of CD38, CD49d and TLR9 established in the total CLL cell population. Using this gating strategy, there is minor correlation between the MFIs of TLR9 with CD38 and none with CD49d.

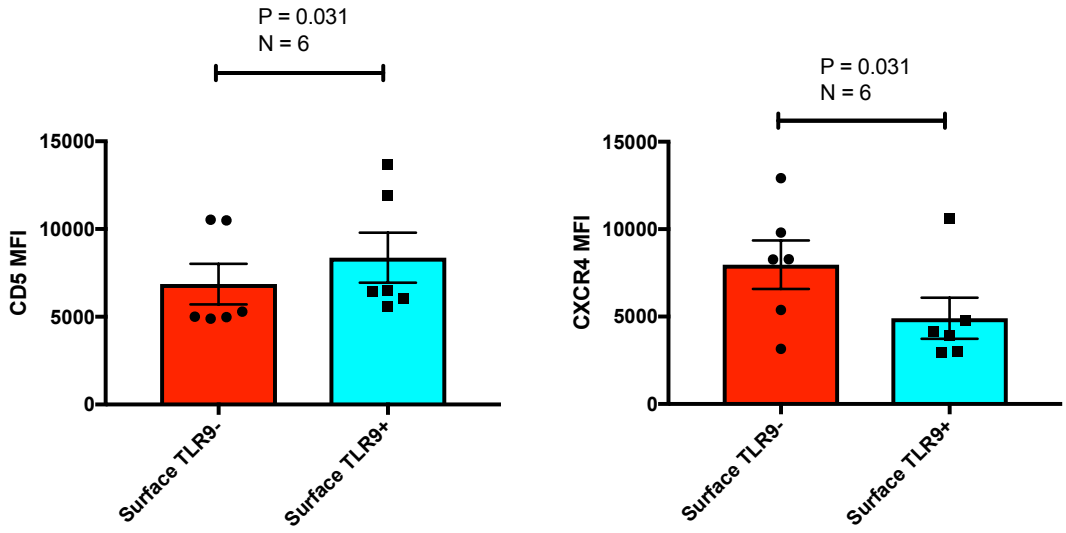

Supplementary Figure 4: sTLR9 positive CLL cells have lower levels of CXCR4 and higher CD5. Unstimulated primary PBMCs from 6 CLL patients were stained with antibodies to CD5, CD19, CXCR4, surface TLR9 and a viability dye. Cell were assessed by flow cytometry. Within each patient's gated CLL cell population, the sTLR9 positive and negative populations were gated on and the MFI of CD5 and CXCR4 established. Within every patient, CXCR4 was lower and CD5 higher in the sTLR positive population compared to their negative counterparts.

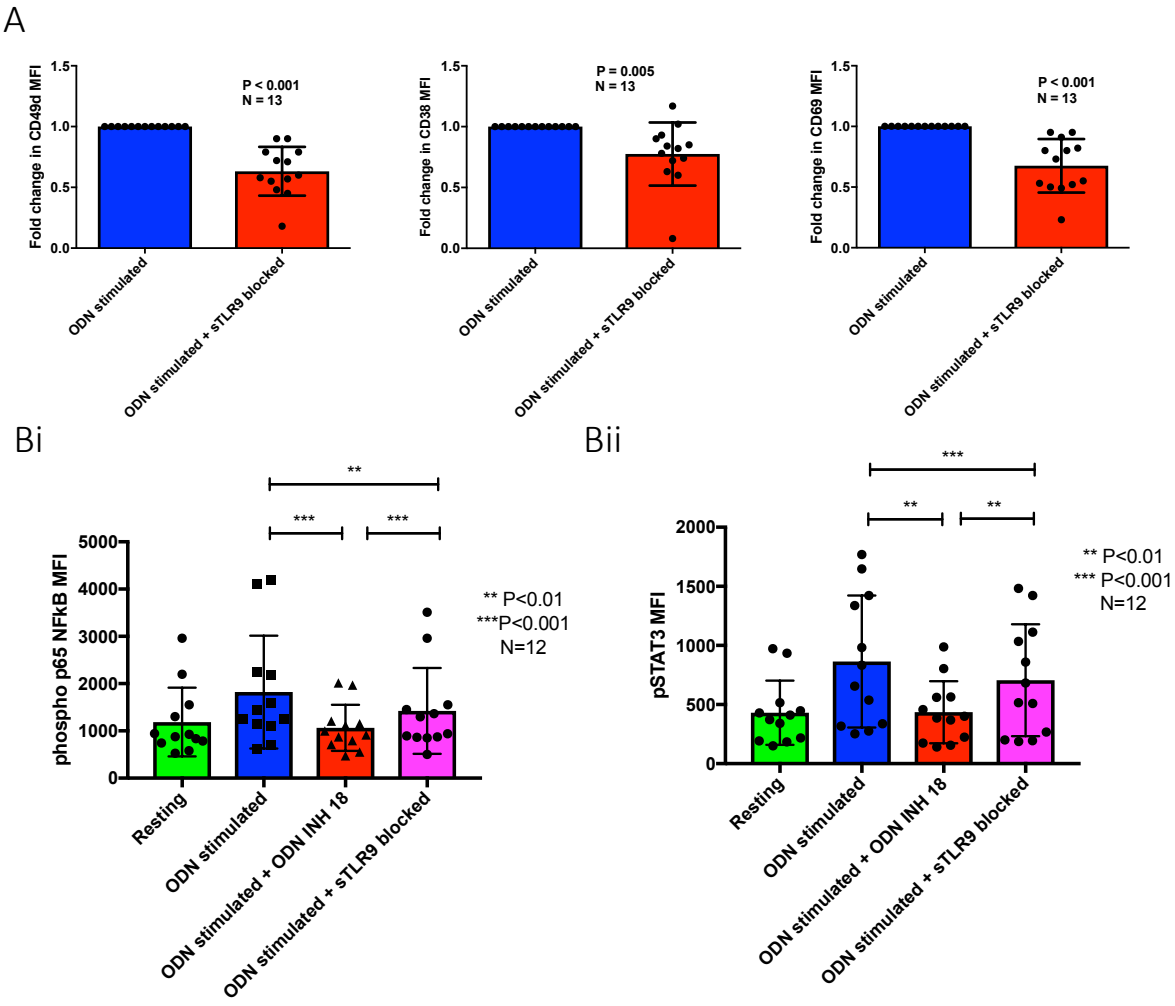

Supplementary Figure 5: Blockade of sTLR reduces ODN-mediated upregulation of CD49d, CD38 and CD69.

(A) PBMCs from 13 different CLL patients were split into two fractions and one fraction was pre-incubated with an antibody to block surface TLR9. Both fractions of cells were then stimulated with ODN2006 overnight. PBMCs were then stained with antibodies to CD5, CD19, CD38, CD49d, CD69 and a viability dye. Viable CD5+CD19+ CLL cells were gated on and the MFI of the other indices assessed. Due to the variation in MFIs, the ODN2006 stimulated-alone results were normalized to 1 and the sTLR9 blocked fraction results presented as a fold change from this. Blocking surface TLR9 reduced the upregulation of CD49d and CD69 in all 13 cases and CD38 in 11/13 cases. **(B)** PBMCs from 12 different CLL patients were split into four fractions. One fraction was pre-incubated with an antibody to block surface TLR9 and one with ODN INH18 to block eTLR9. Both these fractions of cells, and an untreated fraction, were then stimulated with ODN2006 for 4 hours. The fourth fraction remained unstimulated. Cells were collected, stained with CD5, CD19 and either IMC, (i)p-p65 NF-κB or (ii) pSTAT3. p-p65 NF-κB and pSTAT3 MFIs were quantified. Both were upregulated in the presence of ODN2006 and this was very marginally reduced with sTLR9 blocking but much more with eTLR9 blockade.

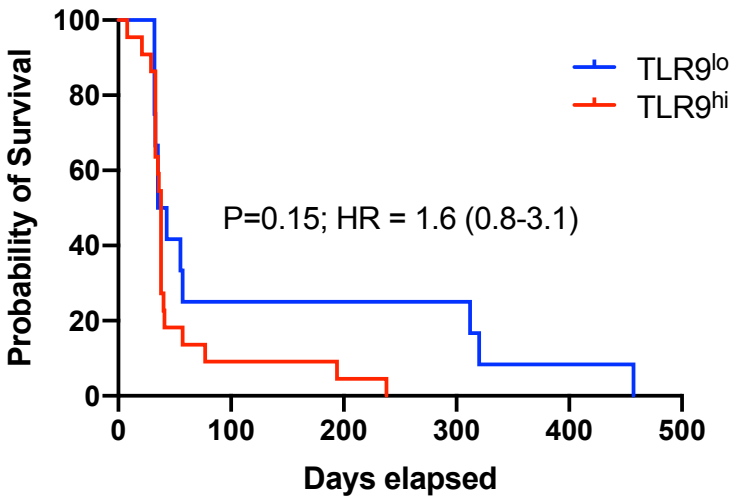

Supplementary Figure 6: Mice engrafted with TLR9^{hi} CLL cells have worse survival than those engrafted with TLR9^{lo} CLL cells.

CLL cells from 7 Patients were segregated into TLR9^{hi} (red) or TLR9^{lo} (blue) and engrafted into 7 groups of mice. Murine condition and survival was monitored, and they were euthanised upon development of the symptoms described above. Although not statistically significant due to low numbers, there is a trend towards better survival when engrafted with TLR9^{lo} CLL cells compared with TLR9^{hi} with a hazard ratio (HR) of 1.6.

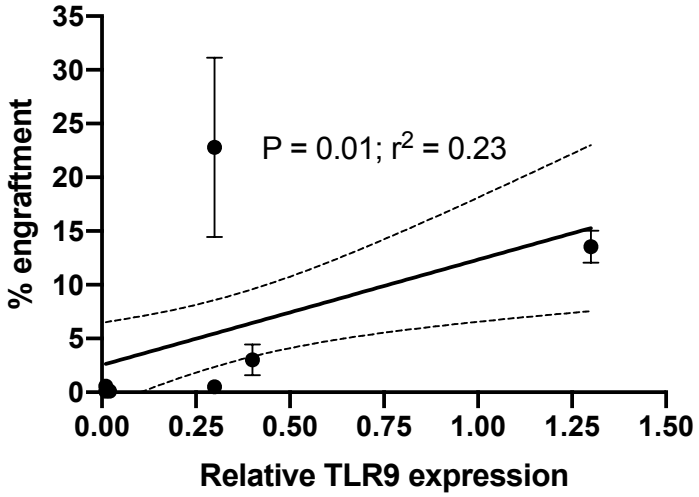

Supplementary Figure 7: Levels of splenic engraftment correlate with levels of TLR9 expression.

CLL cells from 7 Patients were engrafted into 7 groups of mice. The mean % engraftment for each group was plotted against the relative TLR9 expression in the CLL cells from each patient. There is a positive correlation between TLR9 expression and % engraftment.

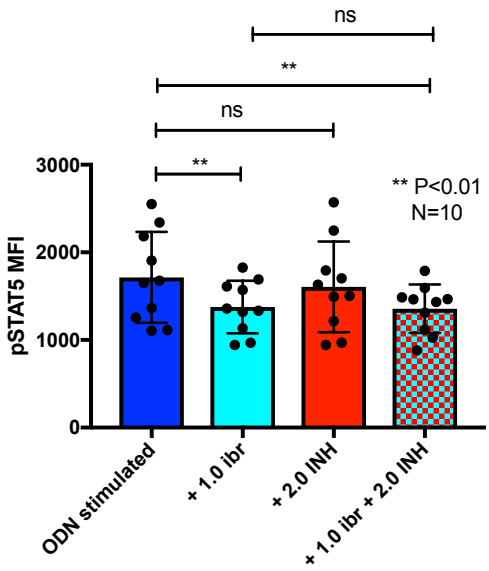

Supplementary Figure 8. Blocking TLR9 is not synergistic with ibrutinib for reducing p-STAT5. PBMCs from 10 different patients were split into 4 fractions. One fraction was stimulated with ODN2006 alone, one fraction stimulated in the presence of ibrutinib, one fraction stimulated in the presence of the TLR9 inhibitor ODN INH-18 and one fraction stimulated in the presence of both (2:1 fixed molar ratio of ODN INH-18 to ibrutinib). Following a 4-hour incubation, cells were harvested and stained for CD5, CD19 and intracellular p-STAT5 or an IMC and then assessed by flow cytometry and the MFI recorded. Only ibrutinib alone marginally inhibited p-STAT5 and this was not altered by the presence of ODN INH-18 .